

COMPOSITE FLEXIBLE INSULATION FOR THERMAL PROTECTION OF SPACE VEHICLES

Demetrius A. Kourtides and Huy K. Tran

Ames Research Center

Moffett Field, CA 94035-1000

S. Amanda Chiu

Sterling Software, Inc.

Palo Alto, CA 94627

NASA

527-18

4.13.87

p 16

SUMMARY

A composite flexible blanket insulation (CFBI) system considered for use as a thermal protection system for space vehicles is described. This flexible composite insulation system consists of an outer layer of silicon carbide fabric, followed by alumina mat insulation, and alternating layers of aluminized polyimide film and aluminoborosilicate scrim fabric. A potential application of this composite insulation would be as a thermal protection system for the aerobrake of the Aeroassist Space Transfer Vehicle (ASTV). It would also apply to other space vehicles subject to high convective and radiative heating during atmospheric entry. The thermal performance of this composite insulation as exposed to a simulated atmospheric entry environment in a plasma arc test facility is described. Other thermophysical properties which affect the thermal response of this system are also described. Analytical modeling describing the thermal performance of this composite insulation is included. It shows that this composite insulation is effective as a thermal protection system at total heating rates up to 30.6 W/cm^2 .

INTRODUCTION

Composite flexible blanket insulation (CFBI) is multilayer insulation consisting of ceramic fabrics, insulation, and reflective foils that are separated by ceramic scrim cloths. A potential application for such multilayer insulations would be as a thermal protection system for the aerobrake of the Aeroassist Space Transfer Vehicle (ASTV). Depending on the exact location of the insulation on the aerobrake, this insulation would be exposed to heating rates up to approximately 31 W/cm^2 (ref. 1).

The maximum heating rate will be reached at approximately 100 seconds into the heating pulse. The multilayer insulation exposed to these heating rates would reach maximum backface temperature at approximately 200 seconds at which time the pressure is essentially that of space. Multilayer insulation is intended for use in the space vacuum where gas conductivity between the foils is negligible and the overall effective thermal conductivity is very small. This appropriately designed multilayer insulation could operate efficiently within the heating and pressure environment of the ASTV, providing a weight saving compared to other types of insulation. In order to demonstrate the effectiveness of this insulation in a typical ASTV flight environment, it is planned to install and fly this type of insulation on the aerobrake of a precursor of the ASTV called Aeroassist Flight Experiment (AFE) (ref. 2).

DESCRIPTION OF MATERIALS

A description of a typical composite flexible blanket insulation is given in figure 1. The composite insulation consists of an outer layer of silicon carbide fabric, followed by an alumina insulation and alternating layers of aluminized polyimide films. It also includes aluminoborosilicate scrim cloths and a bottom layer of aluminoborosilicate fabric. The entire insulation is sewn with a silicon carbide thread.

Some of the properties of the components in this composite flexible blanket insulation are shown in table 1. The overall thermal performance of this insulation is greatly dependent on the thermo-physical properties of the components and the physical arrangement of the components to form the insulation system. Heat transfer in multilayer insulations usually occurs through conduction, convection, and radiation. For space or vacuum applications, the convection mechanism may be neglected as the gas phase is at a greatly reduced pressure. The heat transport processes which are to be considered are conduction through the solid phase of the insulation and radiation. The radiation becomes the dominant mechanism as temperature increases, whereas conduction determines the lower limit of thermal conductivity at lower temperatures. The multilayer insulations have a very small separation such as scrim cloth between the foils. An approximation of the total heat transfer in the full configuration may be estimated by treating the individual components independently. The total heat flux, \dot{q} , through this type of insulation may be expressed as follows:

$$\dot{q}(\text{total}) = \dot{q}(\text{radiation}) + \dot{q}(\text{gas conduction}) + \dot{q}(\text{solid conduction}) \quad (1)$$

The design of the composite insulation shown in figure 1 was based primarily on the theory of equation (2) that describes the heat transfer in multilayer insulations. This equation (ref. 1) is as follows:

$$K_e = BK_s D_f n + \frac{(r)^2 G(T_F^2 + T_B^2)(T_F + T_B)t}{(a + 2s)(t/2) + (N - 1)[(2/E) - 1]} + \frac{(L)}{(L + I)} (K_g) \quad (2)$$

where

K_e	effective thermal conductivity of insulation
B	solid fraction in insulation
K_s	thermal conductivity of solids
D_f	fiber diameter
n	exponent
r	index of refraction
G	Stefan-Boltzman constant
T_F	temperature on front side
T_B	temperature on back side
t	thickness of insulation
L	cell length in insulation
a	absorption cross section
s	scattering cross section
N	number of metal foils
E	emittance
I	mean free path of gas
K_g	thermal conductivity of gas

Equation (2) was used as a guide for the selection of materials and geometry of the composite insulation. It shows the importance of some of the properties of the components and geometry in the multilayer insulations. For example, to achieve lower thermal conductivity in the entire system, a larger number of foils having a low emittance at elevated temperatures is desired. The foils should be placed in the composite where T_F and T_B are relatively small. A small fiber diameter is desired in the insulation as well as low thermal conductivity of the components. Equation (2) shows the influence of the optical properties of both the insulation and foil materials and the number of foils. It also shows the physical and thermal properties of the components (such as density and thickness of insulation), fiber diameter, and the boundary temperatures on the heat transfer properties of the multilayer assembly.

Using these parameters and previous tests (refs. 2 and 3) as guides, the multilayer insulation shown in figure 1 was fabricated and its heat transfer properties evaluated. The reflective shield used in this insulation is a polyimide film with a chemical vapor-deposited aluminum film approximately 800 micrometers thick. As shown in the above equation, a low emittance is desired in the reflective shield. The emittance of this film up to 673 K is approximately 0.05 (ref. 4). The low emittance and high reflectance lead to the effectiveness of these films as a radiation shield in the heating environment of the AFE vehicle. The expected peak heating rate at this environment is approximately 30.6 W/cm^2 consisting of approximately 4.7 W/cm^2 radiative heating and 25.9 W/cm^2 convective (ref. 5). The total heating and pressure rate to which these insulations will be exposed in the space environment is shown in figure 2. As shown, the surface of the insulation will reach the maximum heating rate at approximately 100 seconds. It will be maintained at this rate for approximately 50-60 seconds, after which time both the heating rate and pressure decrease. The "Nominal" and "3-sigma" surface temperature profiles of the AFE Aerobrake at the CFBI location is shown in figure 3. This temperature is the surface temperature on the fibrous refractory composite insulation/ reaction cured glass (FRCI/RCG) at this location. The purpose of the composite flexible insulation is to provide thermal protection to the aluminum substructure when exposed to the heating and pressure environment shown in figure 2. As a guideline, the maximum acceptable temperature limit for the aluminum substructure has been defined as 445.5 K (ref. 1).

The apparent thermal conductivity of the composite flexible insulation shown in figure 1 was determined using the procedure described in reference 6. The apparent thermal conductivity as a function of temperature at three different pressures is shown in figure 4. The thermal conductivity of the alumina insulation used in the CFBI is also shown in the same figure. The thermal conductivity of the CFBI is lower than that of the alumina insulation at lower temperatures but slightly higher at higher temperatures. This could be attributed to the silicon carbide fabric and thread. In addition, the heating in this test method is entirely convective.

TEST RESULTS

One of the objectives of the AFE is to determine the thermal response of this type of insulation under the AFE environment. Another objective is to compare with state-of-the-art rigid thermal insulations such as the fibrous refractory composite insulation (FRCI) coated with a reaction cured glass (RCG) coating described previously (refs. 7-9). FRCI is considered as the baseline tile for the heating region where the composite flexible insulation will be located. The purpose of the tests reported here was to attempt to simulate, as closely as possible, the temperature and heating rate conditions of the AFE trajectory in a test facility. Another purpose is to determine the thermal response of these composite insulations under this environment. The test facility utilized was the NASA Ames 20-MW Plasma Arc Facility described in reference 9. Three radiation equilibrium temperature conditions were used to evaluate the insulations. These temperatures were based on three different heating rates resulting from three different trajectories. These heating rates are 30.6 W/cm^2 for a "nominal" condition, 35.2 W/cm^2 for a "3-sigma" condition and 39.7 W/cm^2 for a "peak heating rate" condition.

These conditions represent the surface temperatures resulting from the "Nominal" and "3-sigma" trajectories of a 1857 kg AFE vehicle and the temperature resulting from the "Peak Heating Rate" of

a 2038 kg AFE vehicle (ref. 10). The model used to establish the test conditions consisted of an FRCI tile approximately 9 cm × 2.5 cm thick installed in the center of another FRCI holder approximately 16 cm in diameter × 5 cm thick. These test conditions produced the FRCI tile surface temperature profiles shown in figure 5. The center rigid model was subsequently replaced with the composite flexible insulation of the same dimensions in the larger holder. The purpose of the larger holder was to reduce any side heating effects on the insulation during testing. The flexible insulation was bonded on the bottom side with a silicone adhesive to an aluminum plate 0.08 cm thick.

The rigid calibration model was instrumented with three thermocouples located, within the RCG coating, on the surface of the tile. The composite flexible insulation test model shown in figure 6, was instrumented with a thermocouple encased in alumina tubing and bonded, with alumina adhesive, on the underside of the top fabric shown in figure 1 and described in table 1. A second thermocouple was installed within the silicone adhesive, between the bottom fabric of the CFBI and the aluminum plate. Both thermocouples were located on the geometric center of the CFBI model.

The surface temperature profiles for the FRCI/RCG calibration model are shown in figure 6. The temperature profiles achieved were fairly close to the targeted temperature profiles shown in figure 3 except for the “heat-up” rate, which is very rapid in the test. The models were inserted in the plasma arc stream for 120 seconds, which is slightly longer than the time of the peak temperature of the AFE. The pressure in the arc jet test chamber was maintained at 0.27 Pa (0.004 psi) during the test model exposure in the arc stream. Subsequently, it was increased in three (3) stages for 440 seconds during the “cool down” of the model to approximate the pressure profile of the AFE space vehicle. The equivalent FRCI/RCG heating rates achieved for the three test conditions were 30 W/cm², 35 W/cm² and 39 W/cm² respectively.

The thermal response of the composite flexible blanket insulation at the 30 W/cm² test condition is shown in figure 7. The surface temperature is the temperature recorded from a Type R thermocouple encased in alumina tubing and bonded on the bottom side of the silicon carbide fabric. The backface temperature is the average temperature recorded by two Type K thermocouples placed within the silicone adhesive. The surface temperature is higher than the FRCI/RCG surface temperature shown in figure 6 at equivalent test conditions. This is attributed to the lower emissivity of the top fabric and other factors such as fabric design and texture. No visual degradation was observed in the fabric. The maximum surface temperature attained was 1850 K. The maximum backface temperature attained was 450 K at 230 seconds. This is within the design limit for the aluminum structure of the AFE vehicle.

The thermal response of the same insulation at the 35 W/cm² test condition is shown in figure 8. This test condition represents the “3-sigma” trajectory of the 1857-kg AFE vehicle. The maximum surface temperature was 1900 K and the maximum backface temperature was 500 K at 230 seconds after the model insertion in the arc stream. Again, the surface temperature is considerably higher than the FRCI/RCG surface temperature. No visual degradation of the surface fabric was observed except for some slight discoloration. The back aluminum plate in the test insulation was 0.08 cm thick. The aluminum skin on the aerobrake is the same thickness, but it is supported by aluminum stringers resulting in an effective thickness of 0.28 cm thick. A thicker backplate in the test model could have resulted in a lower backface temperature since it would act as a heat sink.

The thermal response of the insulation at the 39 W/cm^2 condition is shown in figure 9. The surface temperature reached 1750 K and the backface 580 K at 200 seconds. The surface fabric was removed during testing at some locations possibly due to oxidation and tensile failure of the yarn. This test condition exceeds any of the 1857-kg vehicle trajectory conditions and is not likely to be encountered in flight.

ANALYTICAL MODELING

As stated previously, the composite flexible blanket insulation was instrumented on the surface with a thermocouple probe. The probe consisted of a thermocouple inserted in an alumina tubing bonded to the silicon carbide fabric. The purpose of the tubing is to protect the thermocouple during the thermal exposure and to assure full contact with the surface of the fabric.

Simulation models were developed using the system improved numerical differencing analyzer (SINDA) program (ref. 11) to analyze the thermal responses of both the CFBI insulation and the thermocouple probe. The specific objectives were to predict the in-depth temperatures of the CFBI when exposed to the nominal AFE trajectory and to correlate the temperatures measured by the thermocouple probe to those of the SiC surface.

The models assume an imposed heat flux history at the front surface. Heat is then reradiated to the surrounding blanket as well as conducted through the blanket. The remainder of the heat produces changes in material temperatures. The emissivity of SiC at high temperature has not been well characterized. For these calculations, it was assumed to vary between 0.86 at 311 K and 0.48 at 1839 K (ref. 12). The conductivity of CFBI with silica batting used in the analysis is shown in figure 10, as a function of both temperature and pressure. The models linearly interpolate or extrapolate the thermal properties as required. The backface of the aluminum was taken to be adiabatic. It should be noted that the model did not include the multifoil assembly due to its complexity, which results in conservative calculation of the backface temperature.

A one-dimensional SINDA model was used to determine the in-depth temperature response of CFBI. Figure 11 is a schematic of the model components, including the SiC fabric, alumina batting, RTV and aluminum skin. Figure 12 shows the surface, in-depth, and backface temperatures calculated for the nominal AFE aerothermal environment shown in figure 2. The calculated backface temperature reaches a maximum of 440 K, which is within the aluminum temperature limit of 450 K. The backface of the test sample exposed to the 30 W/cm^2 test condition reached a maximum backface temperature of 450 K, indicating a good correlation of the experimental and calculated results.

Because of the thermal inertia and insulation effects of the alumina probe, the temperature measured by the thermocouple lags the surface temperature. This phenomena was evident from experimental arc-jet results. A three-dimensional SINDA model was developed and used to study the thermal response of the thermocouple probe and to correlate its temperature to the SiC fabric temperature. Figure 13 details the geometry and components of the model.

Comparisons were made between the calculated thermocouple temperature against the experimental data in order to validate the three-dimensional model. However, the actual heat fluxes to which the test sample was subjected were not directly available. Instead, the heat fluxes were calculated by using the RCG temperatures measured from the calibration test, since the thermal physical properties of the RCG and FRCI are well established (ref. 8). Using a constant RCG emissivity of 0.85 and assuming the measured RCG temperatures were at radiation equilibrium, the heat fluxes were then calculated.

After the heat fluxes had been established for the test conditions, they were then imposed onto the three-dimensional model. The model simulates the thermal response of the thermocouple probe embedded in the CFBI. Figure 14 compares the calculated thermocouple probe temperatures to the empirical values. The results indicated that the model predictions correspond well with the measured values. However, the model predictions still lag behind the actual measurements. The discrepancy was probably due to the difference between the conductivities used in the analysis and those of the actual insulation material. Another possible cause is the added thermal mass of the adhesive used to secure the probe. Further refinement of the model will be carried out. Figure 14 also shows the calculated top surface temperatures at a location away from the thermal effect of the probe. As expected, the SiC temperatures respond significantly faster than the probe temperatures.

CONCLUSIONS

The thermal properties of a lightweight composite flexible blanket insulation suitable for the Aeroassist Space Transfer Vehicle environment were reviewed. This multilayer type insulation provides thermal protection to an aluminum structure when exposed to a heating environment similar to that of the aerobrake of the Aeroassist Flight Experiment. No visual failure of the insulations is observed when the insulations are exposed to a plasma arc test condition which produces a surface temperature of 1645 K on an FRCI/RCG rigid insulation. The surface temperature of the insulation is higher and this is attributed to the lower emissivity of the silicon carbide fabric. The ability of the thermal analysis models to predict the temperature responses of these insulations was demonstrated. Further refinements to these models are being carried out. They will be utilized in the future to aid analyses of the temperatures obtained during the actual AFE flight.

REFERENCES

1. Aeroassist Flight Experiment Carrier Thermal Environments Data Book, NASA-MSFC-DOC-1607, 1989.
2. Viskantan, R.: Heat Transfer by Conduction and Radiation in Absorbing and Scattering Materials, *J. Heat Transfer (ASME)*, 1965.
3. Pitts, W. C.; and Kourtides, D. A.: Ceramic Insulation/Multifoil Composite for Thermal Protection of Reentry Spacecraft, Proc. of the AIAA 24th Thermophysics Conference, Buffalo, NY, 1989.
4. Thermal Control Materials and Metalized Films, Tech. Bull. No. 3-86, Sheldall Corp., March 1986.
5. Rochelle, W. E.: AFE Aerobrake Aerothermodynamic Data Book, NASA-JSC-23623, Oct. 1990.
6. ASTM C-177-85, Steady State Heat Flux Measurements and Thermal Transmission Properties by Means of the Guarded Hot Plate Apparatus.
7. Goldstein, H. E.: Fibrous Ceramic Insulations, NASA CP-2251, Nov. 1982.
8. Stewart, D. A.; Goldstein, H. E.; and Leiser, D. B.: High Temperature Glass Thermal Control Structure and Coating, U.S. Patent 4381333 (April 1983).
9. Leiser, D. B.; Smith, M.; and Stewart, D. A.: Options for Improving Rigid Ceramic Heat-shields, *Am Ceramic Soc. Bull.*, 1985.
10. Aeroassist Flight Experiment Aerobrake Thermal Design Book, NASA Rep. JSC-23571, May 1989.
11. Cullimore, B.; Goble, R.; Jensen, C.; and Ring, S.: SINDA '85/FLUINT, Systems Improved Numerical Differencing Analyzer and Fluid Integrator, Martin Marietta Corp., Denver, CO., Aug. 1986.
12. Sawko, P.: Tailorable Advanced Blanket Insulation, Presented at joint NASA/Clemson University Conference, Greenville, SC, Nov. 3-6, 1987.

Table 1. Typical properties of components in composite flexible blanket insulation.

Component	Thickness, cm	Density, g/cm ³	Area density, g/m ²	Specific heat, kJ/kg K	Thermal conductivity, W/m K
Silicon carbide fabric 5 harness satin weave Yarn count 1260 warp × 670 Fill/m, 1.5×10^3 Filaments/m ² Fiber diameter, 9 μm	0.065		570		0.664 along fiber axis at 300 K at 101.3 kpa
Alumina mat (95% Al ₂ O ₃ 5% SiO ₂) Fiber diameter, 3 μm	2.305	0.096	2213	0.336 at 1200 K	0.15 at 1200 K at 101.3 kPa
Aluminoborosilicate fab- ric (62% Al ₂ O ₃ , 24% SiO ₂ , 14% B ₂ O ₃) Fiber diameter, 3 μm	1 ply × 0.33 9 plies × 0.010		258 9 plies × 34		
Aluminized polyimide film	10 plies × 0.007		10 plies × 11		
Aluminoborosilicate fab- ric (62% Al ₂ O ₃ , 24% SiO ₂ , 14% B ₂ O ₃) Fiber diameter, 3 μm	0.109		791		
Silicon carbide thread	0.036		300		
Composite flexible blan- ket insulation assembly	2.61	0.174	4548		0.11 at 1250 K at 101.3 kPa

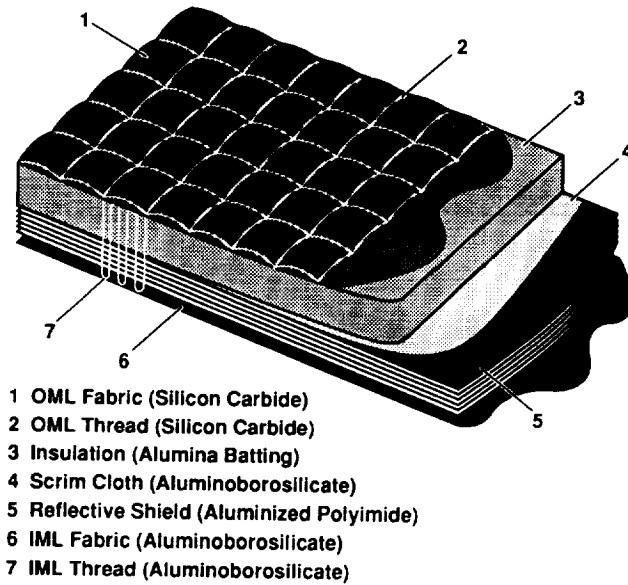


Figure 1. Composite flexible blanket insulation (CFBI).

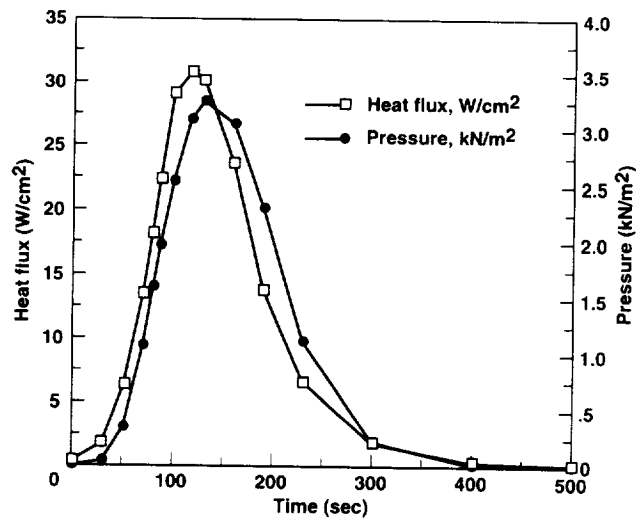


Figure 2. Heating and pressure profiles of the AFE aerobrake at the composite flexible blanket insulation location.

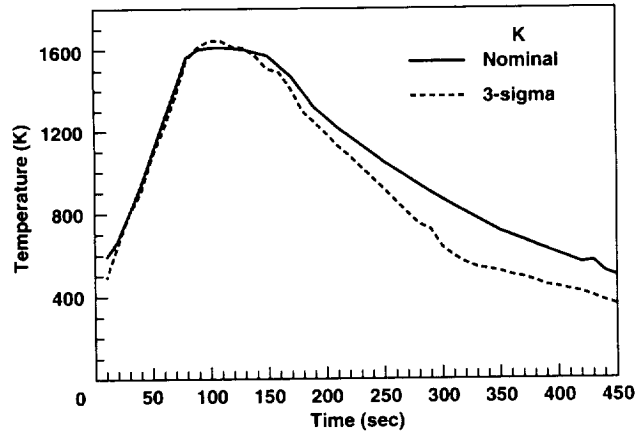


Figure 3. Nominal and three-sigma surface temperature profiles of the AFE aerobrake at the composite flexible blanket insulation location.

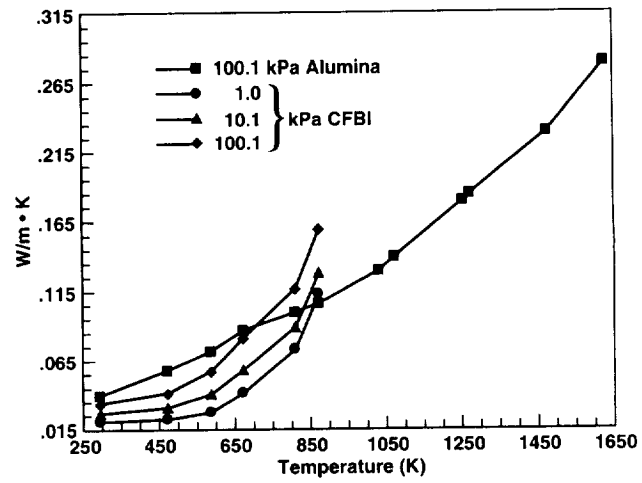


Figure 4. Apparent thermal conductivity of composite flexible blanket insulation.

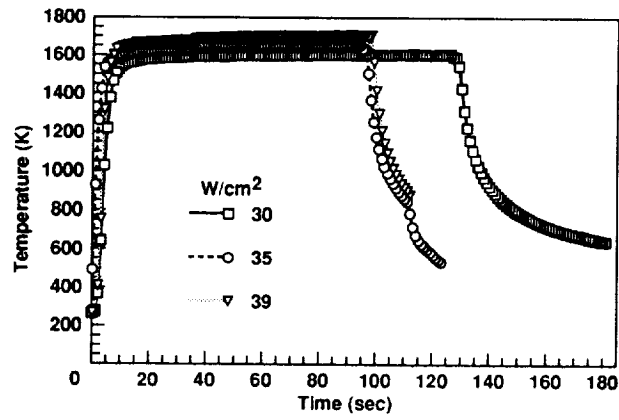


Figure 5. Surface temperatures of fibrous refractory composite insulation/reaction cured glass in the 20 mW Plasma Arc Test Facility.

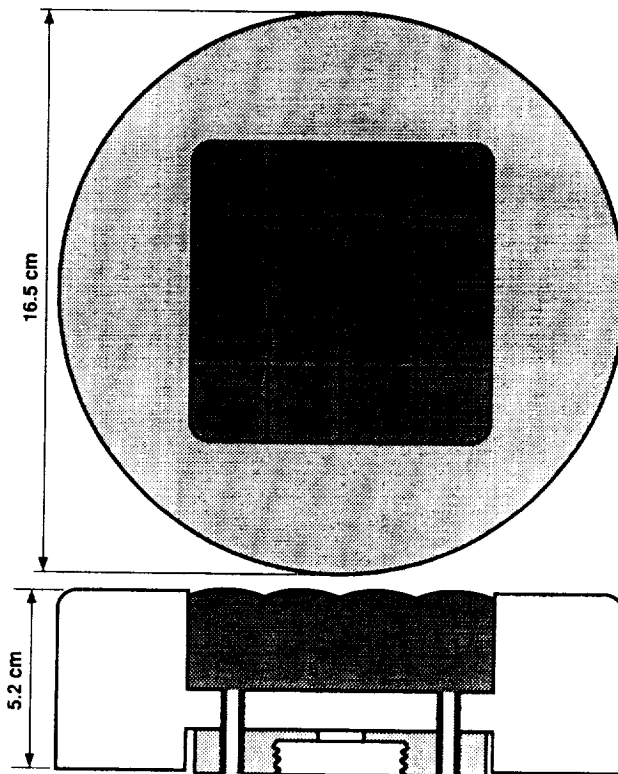


Figure 6. Arc-jet test model for flexible insulation.

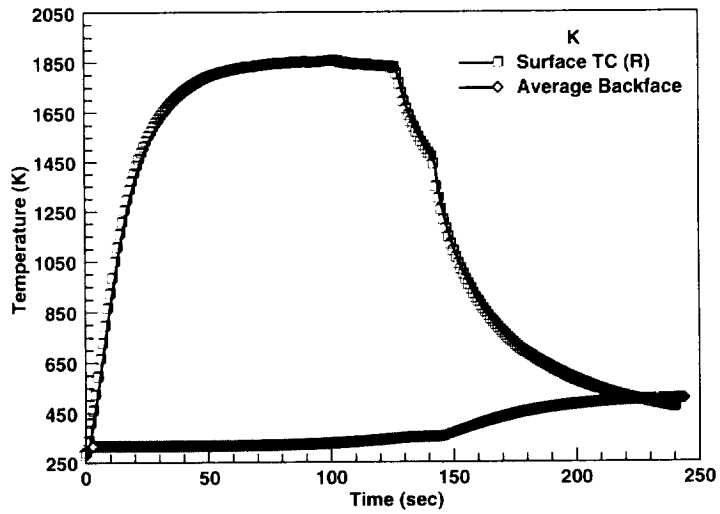


Figure 7. Thermal response of composite flexible blanket insulation at 30 W/cm² test condition in the 20 mW Plasma Arc Test Facility. TC – thermocouple.

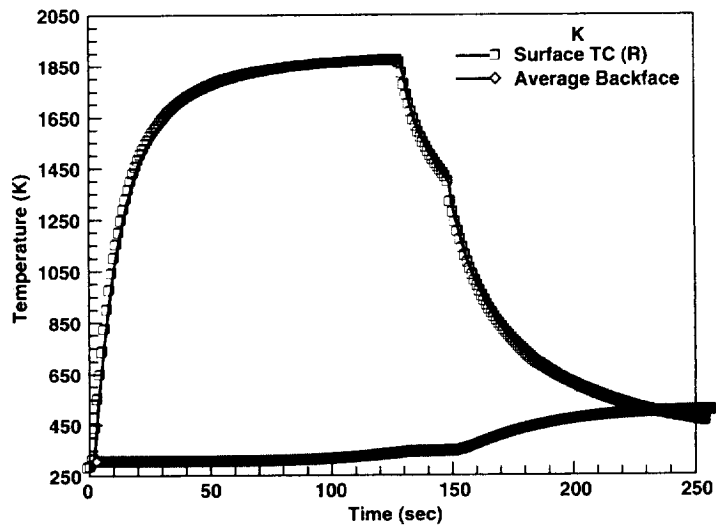


Figure 8. Thermal response of composite flexible blanket insulation at 35 W/cm² test condition in the 20 mW Plasma Arc Test Facility.

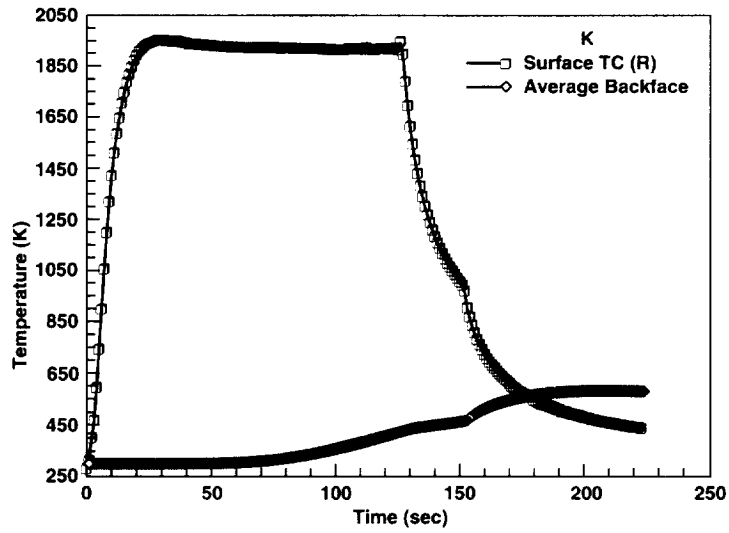


Figure 9. Thermal response of composite flexible blanket insulation at 39 W/cm^2 test condition in the 20 mW Plasma Arc Test Facility.

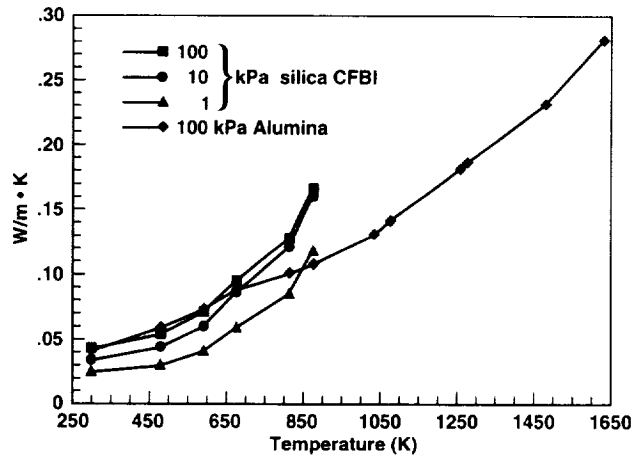


Figure 10. Apparent thermal conductivity of composite flexible blanket insulation (CFBI) with silica batting.

1-D THERMAL MATH MODEL

used for CFBI In-Depth Thermal Conditions

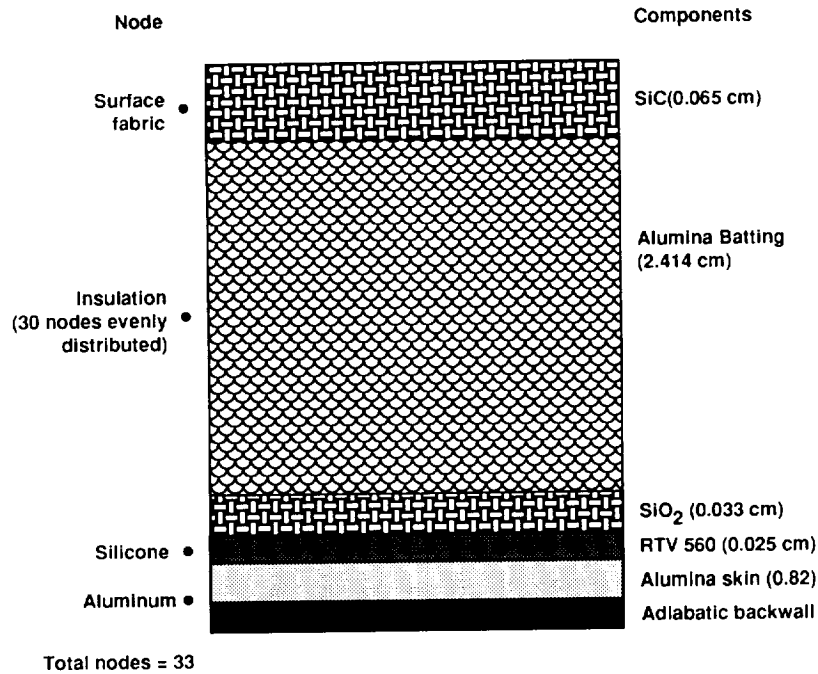


Figure 11. Heat transfer model for composite flexible blanket insulation. RTV – room temperature vulcanizing.

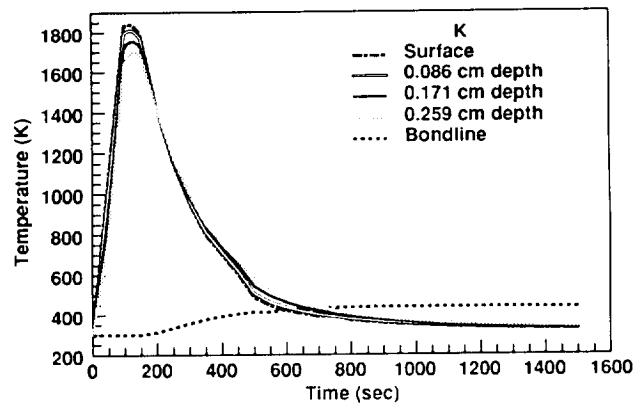


Figure 12. Calculated thermal response of composite flexible blanket insulation during nominal aeroassist flight experiment trajectory.

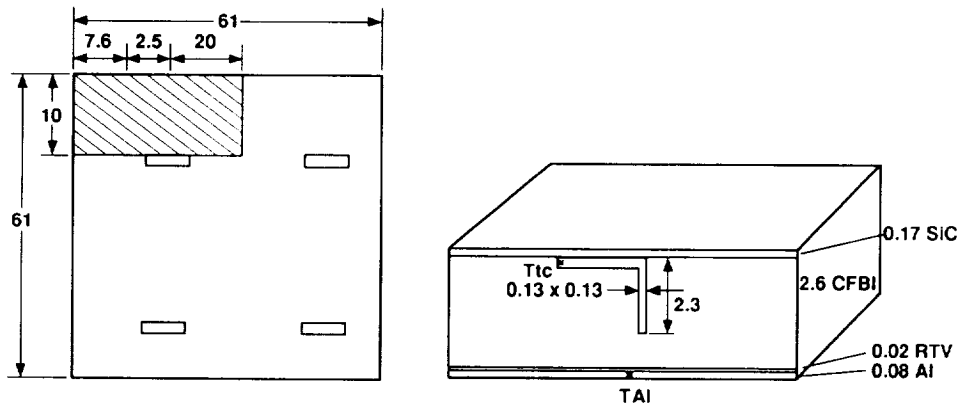


Figure 13. Model geometry of composite flexible blanket insulation with thermocouple probe.

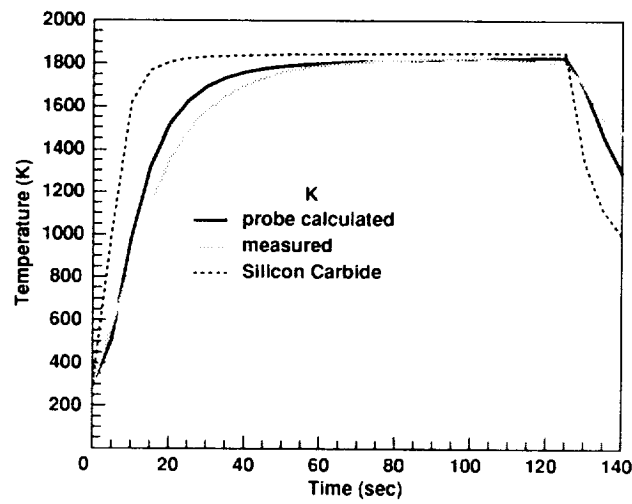


Figure 14. Comparison of calculated and measured surface temperature of composite flexible blanket insulation at 1589 K test condition.